Modulation of GLUT4 and GLUT1 Recycling by Insulin in Rat Adipocytes: Kinetic Analysis Based on the Involvement of Multiple Intracellular Compartments[†]

Wan Lee, Jiwon Ryu, Robert A. Spangler, and Chan Y. Jung*

Biophysics Laboratory, VA Medical Center, and Department of Physiology and Biophysics, School of Medicine, State University of New York at Buffalo, Buffalo, New York 14215

ABSTRACT: The trafficking kinetics of GLUT4 and GLUT1 in rat epididymal adipocytes were analyzed by a four-compartment model based upon steady-state pool sizes of three intracellular fractions and one plasma membrane fraction separated and assessed under both basal and insulin-stimulated states. The steady-state compartment sizes provided relative values of the kinetic coefficients characterizing the rate of each process in the loop. Absolute values of these coefficients were obtained by matching the simulated half-times to those observed experimentally and reported in the literature for both basal and insulin-stimulated states. Our analysis revealed that insulin modulates the GLUT4 trafficking at multiple steps in the rat adipocyte, not only reducing the endocytotic rate constant 3−4-fold and increasing the exocytotic rate 8−24-fold but also increasing the two rate coefficients coupling the three intracellular compartments 2−6-fold each. Furthermore, GLUT1 was completely segregated from GLUT4 in two of the three intracellular compartments, and its steady-state distribution is consistent with a four-compartment model of GLUT1 recycling involving an insulin sensitive endocytosis step in common with the GLUT4 system, but with all other processes being insensitive to insulin.

The uptake of glucose by muscle and adipose cells is catalyzed by the facilitative glucose transporters GLUT4[1] and GLUT1 as the major and minor isoforms, respectively, and further is regulated by insulin as reviewed recently (*1−3*). GLUT4 and GLUT1 in these cells are largely kept idle in intracellular sites, and insulin recruits GLUT4 and GLUT1 from intracellular sites to the plasma membrane, increasing steady-state plasma membrane levels as much as 10- and 2-fold, respectively (*2, 4, 5*). Evidence also indicates that GLUT4 and GLUT1 in these cells constantly and rapidly recycle between the plasma membrane and intracellular sites by endocytosis and exocytosis, and insulin-induced recruitment is associated with modulation of these processes (*6− 8*). In ultrastructural studies, GLUT4 was localized in several, morphologically distinct membrane structures, suggesting the involvement of multiple intracellular compartments in the processes (*9, 10*). The roles of these individual intracellular compartments in GLUT4 and GLUT1 recycling and in their insulin-induced recruitment are currently unknown.

Using hypotonic lysis instead of mechanical homogenization, we (*11*) have recently separated the rat adipocyte intracellular GLUT4 compartments into three distinct fractions, T, H, and L, where T contained all of the plasma membrane in addition to intracellular organelles trapped in it while H and L were exclusively of intracellular organelles with no plasma membrane contamination. In this study, we isolated a plasma membrane fraction (PM) separately by the conventional homogenization and subcellular fractionation method (*12*) and measured its GLUT4 content, which also allowed us to assess the size of the intracellular GLUT4 compartment trapped in T by a simple subtraction. Distribution of various recycling proteins and endosomal markers further suggested that the intracellular GLUT4 in T, H, and L (G4T, G4H, and G4L, respectively) are putative sorting, storage, and exocytotic vesicle compartments, respectively, in the GLUT4 recycling itinerary.

Detailed model studies (*13, 14*) have shown that the GLUT4 recycling kinetics in the adipocyte are inconsistent with a model of one intracellular and one plasma membrane compartment, and proposed a number of more complex models where two or more intracellular compartments participate in the recycling. Having identified and assessed the three distinct intracellular GLUT4 compartments in adipocytes (*11*), we attempted here to extend these model analyses and to identify roles of individual intracellular compartments in the GLUT4 and GLUT1 trafficking kinetics. We simulated the GLUT4 trafficking system using a four-compartment model that consisted of one plasma membrane compartment and three intracellular compartments. By adjusting model parameters to reproduce the experimentally observed behavior of the system, in both the basal state and the state maximally stimulated by insulin, we were able to measure the changes in these kinetic coefficients induced by the action of insulin. We also measured the steady-state

---

* To whom correspondence should be addressed: Biophysics Laboratory, VA Medical Center, 3495 Bailey Ave., Buffalo, NY 14215. Telephone: (716) 862-6540. Fax: (716) 862-6526. E-mail: cyjung@acsu.buffalo.edu.

[1] Abbreviations: GLUT4, glucose transporter type 4; GLUT1, glucose transporter type 1; PM, plasma membranes; NM, nuclear and mitochondria; HDM, high-density microsomes; LDM, low-density microsomes; BSA, bovine serum albumin; PBS, phosphate-buffered saline; SDS−PAGE, sodium dodecyl sulfate−polyacrylamide gel electrophoresis.

distribution of GLUT1 in fractions T, H, L, and PM, in basal and insulin-simulated adipocytes. We show that GLUT1 and GLUT4 are compartmentally completely segregated in H and L fractions, and that the steady-state compartment sizes are consistent with a four-compartment model of GLUT1 recycling in which an insulin sensitive endocytosis step operates in common with the GLUT4 system, but with all other processes being separate and insensitive to insulin.

MATERIALS AND METHODS

Materials. Collagenase (type I) was obtained from Worthington (Freehold, NJ). 1F8 was purchased from Biogenesis Ltd. (Sandown, NH). Horseradish peroxidase-labeled protein A and anti-mouse IgG were from Zymed Laboratories (San Francisco, CA). Antibody against GLUT1 was a generous gift from M. Mueckler of Washington University (St. Louis, MO). Trisacryl beads (Reacti-Gel GF-2000) were from Pierce (Rockford, IL). All other reagents were from Sigma except for where otherwise indicated.

Subcellular Fractionation of Adipocytes. Adipocytes were isolated from epididymal fat pads of male Sprague-Dawley rats and stabilized as described previously (*12*). Subcellular membrane fractions enriched with plasma membranes (PM), nuclear and mitochondria (NM), high-density microsomes (HDM), and low-density microsomes (LDM) were separated after homogenation as described previously (*12*). Subcellular fractions from hypotonically lysed adipocytes were prepared as previously described (*11*). Briefly, adipocyte lysates were centrifuged at $900g$ for 15 min, and the resulting $900g$ pellet (T) was resuspended in 600 μL of NaCl/HEPES buffer [150 mM NaCl, 10 mM HEPES, 1 mM EGTA, and 0.1 mM MgCl$_2$ (pH 7.4)]. The $900g$ supernatant was centrifuged at $185000g$ for 2 h, and the pellet ($185000g$ pellet) was resuspended in 600 μL of NaCl/HEPES buffer. A suspension of the $900g$ or $185000g$ pellet, without or after sonication, was then layered onto 9 mL of a 5 to 30% glycerol gradient prepared in NaCl/HEPES buffer over 400 μL of a 50% (w/v) sucrose pad (height of 10 cm), and centrifuged in a 40.2SW rotor (Beckman) at $60000g$ for 1 h, and 13 fractions were collected from the bottom to the top (P and 1−12). This typically separated GLUT4 into two peaks, a sharp, heavy peak (fractions P, 1, and 2) and a broad, light peak (fractions 3−12). They were separately pooled and designated as fractions T$_H$ and T$_L$ for the $900g$ pellet and fractions H and L for $185000g$ pellet, respectively.

Immunoadsorption. The procedures have been described previously (*11*). Briefly, 1F8 or normal mouse IgG was coupled to Trisacryl beads (Reacti-Gel GF2000, Pierce) at a concentration of 0.7 mg of antibody/mL of resin, according to the manufacturer's instructions. The antibody-coupled beads were quenched with 2 M Tris (pH 8.0) for 1 h, incubated with 2% BSA in PBS [134 mM NaCl, 2.6 mM KCl, 6.4 mM Na$_2$HPO$_4$, and 1.46 mM KH$_2$PO$_4$ (pH 7.4)] for 2 h to prevent nonspecific binding, and washed five times with 1 mL of PBS at room temperature. Fractions T$_L$ and L and sonicated fraction H (100 μg of protein each) were incubated with 30 μL of beads overnight at 4 °C, and unbound supernatants were collected for analysis. Beads were washed five times with 1 mL of PBS at 4 °C, and then the adsorbed material was eluted with SDS (2%)-containing Laemmli buffer without β-mercaptoethanol for 1 h at room temperature.
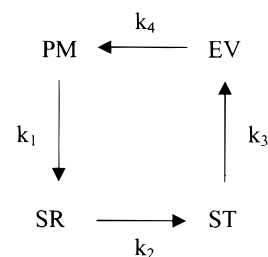

FIGURE 1: Schematic diagram of the four-compartment model: PM, plasma membrane; SR, sorting compartment; ST, storage compartment; EV, exocytotic vesicle compartment; k_i, rate coefficients.

Gel Electrophoresis and Immunoblotting. Solubilized membrane in Laemmli solution was applied to 10% SDS−PAGE resolving gels, and separated proteins were subjected to Western blotting as described previously (*11*). Proteins were visualized using the enhanced chemiluminescent substrate kit (DuPont NEN), and immunoblot intensities were quantitated by densitometry using an analytical scanning system (Molecular Dynamics, Sunnyvale, CA). The protein was quantified with the BCA protein assay solution (Pierce), according to the manufacturer's instructions.

Development of the Four-Compartment Kinetic Model. The structure of the model is assumed to be a simple circular arrangement, as shown in Figure 1. This configuration is consistent with the observation that GLUT4 recycling is a highly regulated, energy-dependent process with distinct donor and target compartments for each step. The four compartments, denoted plasma membrane (PM), sorting (SR), storage (ST), and exocytotic vesicle (EV), each receive inflow from the preceding compartment and, in turn, provide a flow into the following pool. The flow between compartments is assumed to be unidirectional, with a rate that is linearly dependent upon only the content of the source compartment. Although this flow is likely to be mediated by one or more protein functions, we assume that under physiological conditions, the flow rate is well below the saturation level. Embedded energetic reactions driving the flow, as implied by the assumption that each step is irreversible, are not explicitly included in the model.

Thus, by virtue of these assumptions, the flux, J_1, of the process (Figure 1), endocytosis, is given by the simple linear kinetic law

$$J_1 = k_1(PM)$$

where PM is the GLUT content of the PM compartment, expressed as a percentage of the total transporter in the system. The k_i values are rate coefficients in units of reciprocal time, and J_i values are intercompartment transfer rates in units of percent per time. Thus, compartment volumes, and absolute concentrations, do not appear in the kinetic equations. Furthermore, since all kinetic equations are linear, the total amount of GLUT isoform occurs as a common factor in all terms, and hence cancels out, making no contribution to the form of the solution.

The rate of change of the plasma membrane compartment then becomes

$$d(PM)/dt = J_4 - J_1 = k_4(EV) - k_1(PM)$$

and similar equations apply to each of the individual compartments. Although the model system comprises four

compartments, only three are independent since we assume that total GLUT4 or GLUT1 is conserved over the observed time span; thus,

$$PM + SR + ST + EV = 100$$

Four was selected as the number of compartments in the model in accordance with the number of fractions that can be distinguished by the fractionation protocol, and as a number that is sufficiently large to adequately represent the presumed kinetic complexity of the transporter system. Although the real system is probably more complicated, modeling with a greater number of compartments would not be justified in terms of the precision with which the experimental data can be analyzed. For example, a discrete pool representing the endocytotic vesicles, while likely to be a physical reality, does not appear in the model since the content of this pool is assumed to be a negligible fraction of the total GLUT within the system. This assumption is supported by the absence of an observable related fraction in the fractionation procedure (*11*).

Steady-state distribution of GLUT among the four compartments is achieved when the flux of each process is the same, and the time derivative of each pool size vanishes. Under these conditions, a simple relationship exists between the kinetic coefficients and the steady-state level of the pool sizes

$$J_{SS} = k_1(PM)_{SS} = k_2(SR)_{SS} = k_3(ST)_{SS} = k_4(EV)_{SS}$$

where the subscript SS denotes steady-state values. Thus, the *relative* magnitudes of the four rate coefficients can be determined from the steady-state compartment contents. Since the flux is an undetermined quantity, however, the absolute values of these coefficients cannot be deduced solely from steady-state measurements. Consequently, data derived from the time-dependent behavior of the model must be employed for this purpose. By scaling the sets of rate coefficients, such that the experimentally observed and simulated time constants are as similar as possible, we can assign absolute values to the rate coefficients. Separate scaling factors are employed for the basal and insulin-stimulated states, since these two states are kinetically independent.

Boundary Conditions Affecting the Transient Behavior of the GLUT4 Model System. In the analysis of experimental GLUT4 data, we are concerned with two types of time-dependent data. The first, denoted TRAN, is the time course followed by the system upon the sudden change in kinetic parameters from those characteristic of the basal state, to those attained under insulin stimulation, and the converse. The initial values of the pool size in this type of transition are then the steady-state values of the state (basal or insulin-stimulated) occupied by the system just prior to the transition. The second class of time-dependent data, denoted SS, is that generated by labeling the plasma membrane pool with a tracer, and measuring the decrease in PM content resulting from the redistribution of the marker throughout all four compartments. In this instance, the corresponding initial conditions are 100% in PM, and zero elsewhere. Since the system is mathematically linear, the tracer distribution is

independent of the majority component which remains at its steady-state distribution.

Corresponding to the three independent pool sizes characterizing the model system, the time course followed by the system in relaxing into its steady state will, in general, be composed of a weighted linear sum of three characteristic exponential functions. It is important to note that the relative contribution of each of these characteristic exponentials will vary, depending upon the initial conditions imposed upon the system. Consequently, the *apparent* half-time empirically observed for a particular compartment will depend on the type of transient experiment, TRAN or SS, which is being conducted. Experimentally, only the plasma membrane compartment has been assayed with sufficient time resolution to provide useful transient data, and the time course of PM in relaxing into its steady state is usually characterized by a single lumped parameter, an apparent half-time. In like fashion, the curves generated by the model simulation are analyzed in terms of a single, apparent half-time, estimated simply as the period required for the PM pool to relax one-half of the interval to its ultimate value.

It has been assumed, in modeling the transient behavior of the system, that the perturbation resulting in its subsequent relaxation into the steady state is essentially instantaneous. For example, any time delay in the signal transmission from the insulin receptor to the resultant change in kinetic coefficients is ignored in the structure of the model. Further, the possible existence of an occluded portion of the GLUT4 at the plasma membrane, resulting in a difference between carrier amount and glucose transport activity, has not been considered in this model, nor have transport measurement data been used in calibrating the kinetic coefficients.

The simulation procedure utilized in this study consisted of numerical integration of the differential equations describing the kinetic system by means of a second-order predictor–corrector integration algorithm with a fixed step size. The step size was sufficiently small that doubling its magnitude had no effect upon the computed results.

RESULTS

A Comparison of Steady-State GLUT4 and GLUT1 Compartments. Rat epididymal adipocyte intracellular compartments were separated into three fractions (see Materials and Methods), namely, a fraction trapped inside plasma membrane sheets (T) and two plasma membrane-free fractions, H and L. Fraction T was further separated after sonication into fractions T_H and T_L on glycerol gradient centrifugation. A plasma membrane fraction (PM) was prepared by the conventional homogenization–subcellular fractionation method (*12*). We have previously shown that the intracellular GLUT4 pools separated in T, H, and L are distinct and may represent the compartments for GLUT4 sorting (SR), storage (ST), and exocytic vesicles (EV), respectively (*11*).

Here we compared the steady-state distribution of GLUT1 and GLUT4 in these fractions in basal and insulin-stimulated adipocytes by immunoblotting them with GLUT1- and GLUT4-specific antibodies (Figure 2, upper panel). The steady-state GLUT4 and GLUT1 pool sizes in fractions T (T_H plus T_L), H, and L were then calculated from the relative blot intensities and the respective protein yields (Figure 2,

Table 1: Steady-State GLUT4 Contents of Each of the Four Compartments, Rate Coefficients, and Half-Times[a]

	6% basal	ins/bas (6%)	insulin	ins/bas (2%)	2% basal
PM (%)	6 ± 2.0	6	36 ± 1.8	18	2
SR (%)	20 ± 2.8	1	20 ± 3.2	0.83	24
ST (%)	56 ± 3.7	0.72	40.4 ± 2.2	0.72	56
EV (%)	18 ± 1.6	0.2	3.6 ± 0.5	0.2	18
k_1 (min^{-1})	0.380	0.29	0.111	0.27	0.417
k_2 (min^{-1})	0.114	1.75	0.200	5.71	0.035
k_3 (min^{-1})	0.040	2.48	0.099	6.60	0.015
k_4 (min^{-1})	0.127	8.75	1.11	24.0	0.046
	SS	TRAN	SS	TRAN	SS	TRAN
exp $t_{1/2}$ (min)[b]	1.7	(11)	3.2	2.4	1.7	(11)
sim $t_{1/2}$ (min)	1.7	1.5	3.5	1.4[c]	1.7	1.6

[a] PM, SR, ST, and EV signify plasma membrane, sorting compartment, storage compartment, and exocytotic vesicle compartment, respectively, as in Figure 1. The steady-state contents of each of the four compartments are averages of three independent measurements (see Materials and Methods) and are expressed as a percent of total GLUT4, under both basal and insulin-stimulated conditions. Values for SR are obtained by subtracting measured PM values from measured values with T. Shown in the last column are values assuming 2% basal PM as discussed in the text. Rate coefficients are scaled to achieve the best correspondence between the experimental half-times, as reported in the literature, and half-times measured in the simulation. Columns labeled ins/bas show the ratios between the values of each rate coefficient and compartment size in the insulin-stimulated and basal states as derived from the model. Values for exp $t_{1/2}$ shown within parentheses are not used in calibrating the model kinetics; see the text. [b] Values from refs *6, 7, 13,* and *15–17.* [c] Value from the 6% basal initial state; for the 2% basal state, $t_{1/2}$ is 1.6 min.
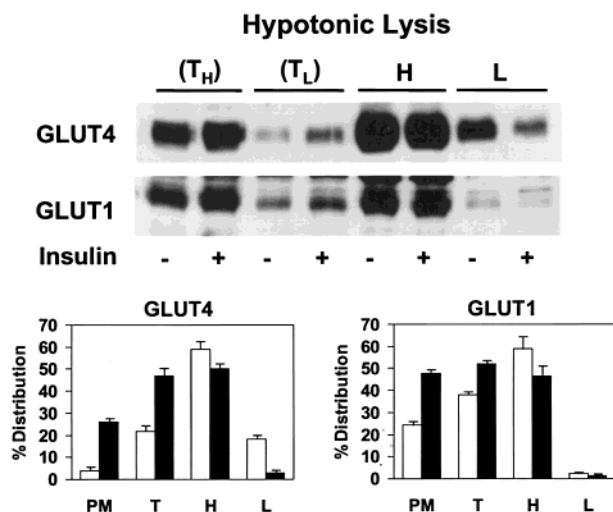
Hypotonic Lysis

FIGURE 2: Subcellular distribution of GLUT4 and GLUT1 in basal ($-$) and insulin-treated ($+$) adipocytes. (Upper panel) Fractions T_H, T_L, H, and L were prepared from basal and insulin-stimulated adipocytes as described in Materials and Methods, and 5 μg of protein from each fraction was subjected to GLUT4 or GLUT1 immunoblotting. The results were reproduced in three additional experiments. (Lower panels) Immunoblot intensities revealed as described above were quantitated by densitometry, and percent distributions of GLUT4 and GLUT1 were calculated after adjustment for protein yields in each fractions. GLUT4 and GLUT1 in T represent those in T_H and T_L. PM denotes the plasma membrane, whose GLUT4 and GLUT1 pool sizes were assessed in parallel experiments using PM, NM, HDM, and LDM fractions (Materials and Methods), and then PM pool sizes were expressed as a percentage of the total cellular contents as discussed in the text. White and black columns represent basal and insulin-stimulated states, respectively, and vertical lines indicate the standard deviation. These results were derived from four independent experiments.

lower panel). For the assessment of the plasma membrane compartment (PM) sizes, similar immunoblotting analyses were repeated using the PM, NM, HDM, and LDM fractions (see Materials and Methods) obtained by the conventional homogenization–fractionation protocol (*12*) (not illustrated). GLUT1 contents in PM were calculated as a percentage of the total in all the fractions, which were included in the analysis (Figure 2, lower panel). Steady-state compartment sizes for PM, SR, ST, and EV were calculated from these data and are summarized in Tables 1 and 2.

Table 2: Measured Steady-State Distribution of GLUT1 among the Four Compartments, Rate Coefficients, and Half-Times[a]

	basal	ins/bas	insulin	insulin (hypoth)
PM (%)	24.4 ± 1.9	1.97	48.0 ± 2.5	52.5
SR (%)	13.6 ± 1.3	0.30	4.1 ± 1.6	8.5
ST (%)	59.8 ± 6.7	0.78	46.5 ± 6.6	37.6
EV (%)	2.2 ± 0.2	0.64	1.4 ± 0.4	1.4
k_1 (min^{-1})	0.380	0.29	0.111	0.111
k_2 (min^{-1})	0.682	2.0	1.333	0.682
k_3 (min^{-1})	0.155	0.73	0.113	0.155
k_4 (min^{-1})	4.22	1.26	5.33	4.22
	SS	TRAN	SS	TRAN	
sim $t_{1/2}$ (min)	1.28	1.28	3.0	3.1	

[a] The values of k_1 in the basal and insulin states are set equal to those for GLUT4. The insulin (hypoth) column shows the insulin stimulated steady-state compartment sizes that would be compatible with the measured basal-state values, if all rate coefficients, other than k_1, were insensitive to insulin.
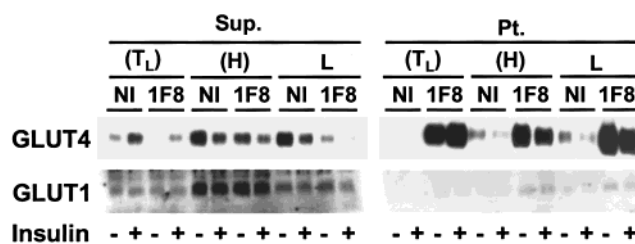

FIGURE 3: Compartmental segregation of GLUT1 and GLUT4 in rat adipocytes. Fractions T_L, H, and L were prepared from basal ($-$) and insulin-stimulated ($+$) rat adipocytes, and subjected to immunoadsorption using 1F8 (1F8) or normal mouse IgG as a control (NI), and the resulting supernatant (Sup.) and immunoadsorbates (Pt.) were immunoblotted using polyclonal antibodies against GLUT4 and GLUT1. Each lane contained a fixed portion [1/20 (GLUT1) and 1/50 (GLUT4) for Sup. and 2/5 (GLUT1) and 1/5 (GLUT4) for Pt.] of supernatant or adsorbates originated from 100 μg of protein from the specified fraction. Similar results were obtained in two other experiments.

We next immunopurified GLUT4 compartments in fractions T_L, H, and L using GLUT4-specific antibody, 1F8, and measured their GLUT1 contents by immunoblotting (Figure 3). It is clear here that GLUT1 is totally excluded from the GLUT4 compartments in fractions H and L (ST and EV) for both basal and insulin-stimulated adipocytes. GLUT1 also

did not colocalize with GLU4 in T_L, a subfraction of T produced by sonic disruption. T_L represents only a small fraction (10−20%) of the GLUT4 pool in T. Very little PM GLUT4 and no GLUT4 in T_H were immunoadsorbed to 1F8 (not shown). Thus, possible colocalization of GLUT1 in GLUT4 compartments in fraction T_H, representing most of the PM and SR compartments, is yet to be examined. The relative contribution of H, L, and T_L pool sizes to the total cellular pool sizes (Figure 2) indicated that as much as 80% (basal cells) and 53% (insulin-stimulated cells) of GLUT4 and more than 60% (basal cells) and 50% (insulin-stimulated cells) of GLUT1 inhabit separate compartments.

Kinetic Analysis of GLUT4 Recycling in a Four-Compartment Model. The identification and partial characterization of three distinct intracellular GLUT4 pools (G4T, G4H, and G4L as SR, ST, and EV, respectively) in addition of the plasma membrane pool (G4PM as PM) (Table 1) led us to propose the four-compartment model for the GLUT4 recycling in the adipocytes, as described in detail in Materials and Methods and depicted in Figure 1. Assessed steady-state compartment sizes available for both the basal and insulin-stimulated states (Table 1) greatly reduce the number of free parameters to be adjusted, and thereby enhance the relevance of the model results to the actual system. The corresponding scaled kinetic constants derived from these steady-state pool sizes, as described in detail in Materials and Methods, are also shown in Table 1. Since there has been some discrepancy in the literature (*6, 7, 13, 15−17*) regarding the PM pool size under basal conditions, two values, 6 and 2%, representative of those reported were considered here. Also shown in Table 1 are observed half-times taken from the literature (*6, 7, 13, 15−17*) under various conditions, compared with the corresponding $t_{1/2}$ values measured in the simulated system based upon the assigned rate coefficients as shown in Table 1.

In insulin-stimulated GLUT4 trafficking, investigators have noted a difference in the apparent $t_{1/2}$ depending upon the experimental conditions, SS or TRAN (*13*). A similar difference in relaxation time is apparent in the simulated results (Figure 4), and a reasonable match between the observed and simulated half-times under both types of experimental conditions can be achieved. This provides additional support for the validity of the model structure we have assumed.

Under basal conditions, however, the model system produces nearly identical half-time values for the SS and TRAN experimental protocols. The values of $t_{1/2}$ reported in the literature, on the other hand, are widely divergent, varying from 1.7 min in the steady-state experiment (*6*) to about 11 min for the insulin to basal transient (*13, 16, 17*). For reasons mentioned in the Discussion, we have chosen the steady-state measurement (1.7 min) for calibration of the kinetics of the system under basal conditions.

Figure 5 shows the computed time course for each of the four compartments during relaxation under the four different experimental conditions, and for both the 6 and 2% (basal PM pool size) models. From these curves, it is evident that the apparent half-time of the PM compartment is nearly the same both in the basal steady-state experiment and in the transition into the basal state from the insulin-stimulated state, whether the 6 or 2% model is considered. As shown in Table 1, these $t_{1/2}$ values range from 1.5 to 1.7 min. In contrast to
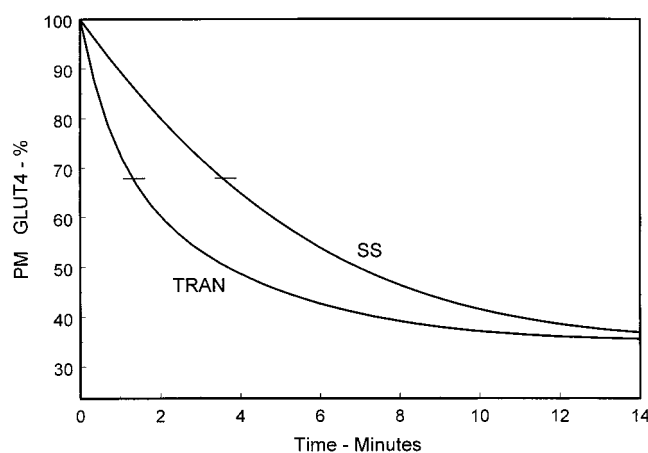

FIGURE 4: Comparison of half-times for PM GUT4 contents for SS and TRAN experimental conditions, in the insulin-stimulated state. The time course for the SS experiment is presented directly, while the TRAN experimental curve is inverted and scaled so as to have the same initial and asymptotic values as the SS curve. Half-time values are 1.4 and 3.4 min for TRAN and SS, respectively, as indicated by crosshatch marks. See the text for the computational procedure.

these results, under conditions of insulin stimulation, the apparent half-times differ by a factor of >2 in the two types of experiments, as shown in Figure 4. In this instance, the apparent $t_{1/2}$ for label redistribution is 3.4 min, compared to 1.4 (6% basal state) or 1.6 min (2% basal state) for the basal to insulin transition.

Undershoot or overshoot in the contents of any single compartment is not unexpected in the four-pool model. As it happens, however, only the sorting compartment, SR, shows a significant overshoot under this particular set of initial conditions that is placed upon the system. Although not immediately evident from the figures, however, the PM compartment also exhibits a slight undershoot, transiently falling below its ultimate steady-state value in both basal-state experiments.

Kinetic Analysis of GLUT1 Recycling in the Four-Compartment Model. With available estimates of steady-state GLUT1 pool sizes of three distinct intracellular compartments and the plasma membrane compartment (Figure 2 and Table 2), a similar kinetic analysis in the four-compartment model for GLUT1 is of interest in comparison to the GLUT4 model results. It is particularly noteworthy that the fractions tentatively identified as the storage and exocytotic vesicle compartments (ST and EV, respectively) for the two GLUT isoforms show no immunochemical overlap between them (Figure 3). A straightforward interpretation of this finding is that, except for the endocytotic step, GLUT1 and GLUT4 are processed through independent pathways. Like many recycling membrane proteins and receptors (*18*), GLUT4 and GLUT1 are shown to be endocytosed via the clathrin-mediated pathway (*7, 9, 10, 19−21*), and it is quite possible that GLUT4 and GLUT1 colocalize in certain endosomal compartments, most plausibly at the putative sorting compartment (SR) (*22, 23*).

On the basis of the concept of an endocytosis process common to both GLUT1 and GLUT4 discussed above, the endocytotic rate coefficient k_1 for GLUT1 is set equal to that of GLUT4 in both the basal and insulin-stimulated states to yield the values shown in Table 2. With this assignment
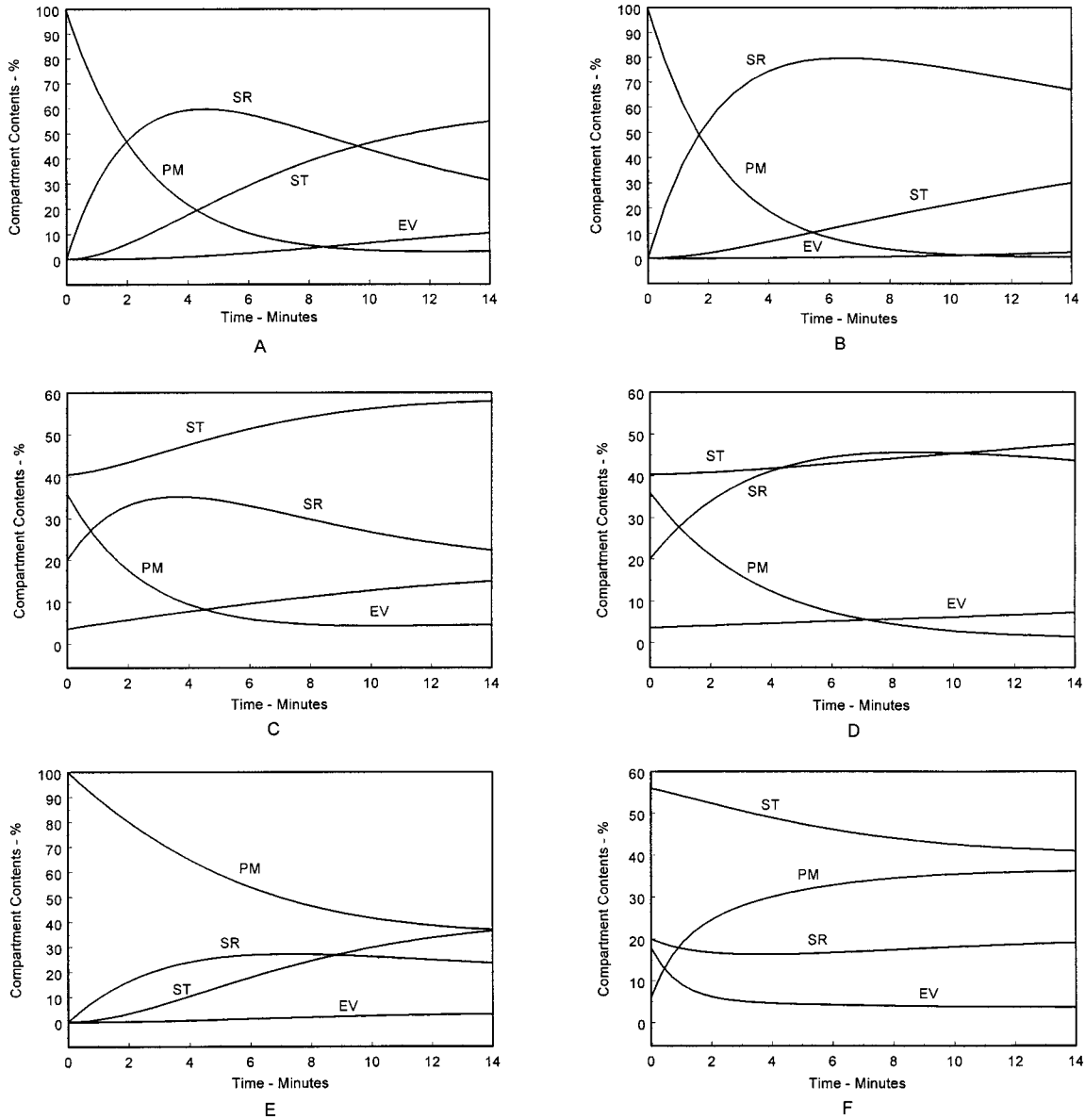
FIGURE 5: Time course, computed by numerical integration of the kinetic equations, for each of the four GLUT4 compartments during relaxation, under both SS and TRAN experimental conditions, and for both the 2 and 6% basal-state models. The SS experiment simulates the redistribution of radioactively tagged GLUT4 introduced into the PM compartment. TRAN experimental conditions in the insulin-stimulated state correspond to the relaxation of the system into its steady state from the 6% basal-state values as initial conditions. Conversely, the insulin-stimulated steady state is the initial condition for the basal TRAN experiment. Refer to the text for the computational procedure. Simulations are for the 6% basal-state SS experiment (A), the 2% basal-state SS experiment (B), the 6% basal-state TRAN experiment (C), the 2% basal-state TRAN experiment (D), the insulin-stimulated SS experiment (E), and the insulin-stimulated TRAN experiment (F).

of k_1 values, together with the measured basal-state pool sizes, it is possible to compute what the insulin stimulated steady-state compartment sizes would be, assuming all rate coefficients of the system, other than k_1, remain constant upon insulin treatment. These values, shown in Table 2 in the column labeled insulin (hypoth), are quite similar to the measured insulin stimulated values, and probably fall within the experimental error of the assay, taking into consideration the possible experimental error in both the basal and insulin-stimulated compartment size measurements. Thus, these data are completely consistent with the mechanistic interpretation that the relatively modest insulin responsiveness of GLUT1 may result from the endocytosis pathway being shared by both GLUT4 and GLUT1, with the remainder of the recycling pathway for GLUT1 being insensitive to insulin effects, as illustrated in Figure 6.
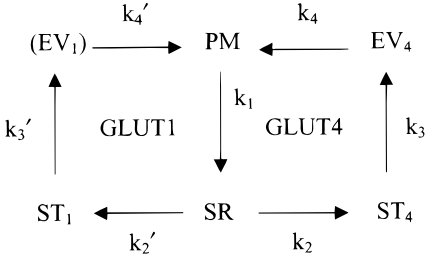

FIGURE 6: Schematic diagram of the GLUT1 and GLUT4 trafficking systems with a common endocytosis step, with all other processes being independent.

DISCUSSION

The GLUT4 compartment sizes assessed here (Figure 2 and Table 1) in each of these fractions for both basal and insulin-stimulated adipocytes closely reproduce those we

have previously reported (*11*). New and interesting findings here are the steady-state GLUT1 compartment sizes in the T, H, and L fractions, which are significantly distinct from those of GLUT4 (Figure 2 and Tables 1 and 2). Most notably, very little if any GLUT1 was found in L, according to the EV compartment analysis (2.2 and 1.4% for basal and insulin-stimulated states, respectively, in Table 2), the fraction that contains the GLUT4 pool significant in size and most sensitive to insulin stimulation (18 and 3.6% of cellular GLUT4 for basal and insulin-stimulated states, respectively, in Table 1). Morphologically, this fraction contains only small vesicles 70 nm in diameter (*11*). For GLUT1, on the other hand, the intracellular compartment trapped in plasma membrane sheets in fraction T (SR in Table 2) is the most sensitive to insulin stimulation (13.6% in basal and 4.1% after insulin stimulation). The intracellular GLUT4 pool size in this fraction (SR in Table 1) was not significantly affected by insulin stimulation. GLUT1 in fraction H (or the ST compartment) is similar to GLUT4 in the fraction; it is by far the largest intracelllular compartment in size and modestly sensitive to insulin stimulation. The plasma membrane GLUT1 compartment amounts to approximately 24% of the cellular GLUT1 in basal adipocytes, which was increased to 48% in insulin-stimulated adipocytes, a 2-fold increase, reproducing values observed with 3T3-L1 adipocytes (*8*).

Our recent estimation of four discrete functional pool sizes in the GLUT4 trafficking system at steady state (*11*) provides the basic configuration of the four-compartment kinetic model (Figure 1). Such data fix the relative values of the rate constants within the model structure. Scaling the absolute values of these coefficients to approximate the kinetic behavior seen experimentally offers insight into the nature of the change produced by insulin stimulation of the system. In constructing this model, we have assumed both unidirectionality and kinetic linearity of the intercompartmental transfer processes as the simplest reasonable representation.

An essential feature of the fitting procedure is that the ratio of half-times observed in the model simulations under the two types of experimental procedure (SS or TRAN) is independent of the scaling parameter, depending instead upon the initial conditions characteristic of the two procedures. Thus, the magnitude of this ratio in the simulated system, when compared with experimentally observed values, provides some indication of the congruence of the model to the physical system. Further evidence supporting the model's structural validity might be provided by the non-steady-state measurement of internal compartment contents (Figure 5). As noted above, the pool identified as SR exhibits a marked overshoot in the model basal-state simulations. Experimental determination of a transient SR pool size well above its ultimate steady-state value would be especially valuable in support of the model, and as a means of more firmly establishing the sequential order of the assay fractions within the recycling sequence.

The $t_{1/2}$ observed for steady-state relaxation in the presence of insulin is about 33% larger than that of the transition from the basal to the insulin-stimulated state (exp $t_{1/2}$ values for the insulin-stimulated state in Table 1). The model generally reproduces this relationship, with a somewhat larger ratio of >2 (sim $t_{1/2}$ values in Table 1 and Figure 5). In part, at least, the difference between these two numbers may result from a delay in signal transmission from the insulin receptor,

thus increasing the apparent half-time of the transition process in the actual system. For this reason, the half-time for the steady-state experiment was considered to be the most accurate representation of the physical system, and this value was weighted relatively more in scaling the model parameter in the insulin-stimulated state.

In the basal state, on the other hand, the half-time ratio evidenced by the kinetic simulations diverges markedly from that reported in the literature. While the model ratio is close to unity, experimental results suggest the transition half-time is about 6.5-fold larger than the $t_{1/2}$ for the steady-state tracer procedure (Table 1). These experimental results are quite possibly misleading, however, because of the undetermined time lag involved in completely flushing insulin and its effects from the system. Accordingly, the $t_{1/2}$ found experimentally in the SS experiment, 1.7 min, was used as a comparison in scaling the model system kinetics to approximate the physical system.

The values of the GLUT4 model kinetic rate coefficients resulting from the fitting procedure (Table 1) have several interesting properties. Under basal conditions, the endocytosis rate constant, k_1, with a value of about 0.4, has a similar magnitude in both the 6 and 2% (basal PM pool size) model variants. In either case, being the largest within the basal set of coefficients, the endocytosis rate constant tends to dominate the kinetic behavior of the PM compartment; in fact, the corresponding time constant τ ($t_{1/2} = 0.693\tau$) of relaxation of the PM content is almost exactly the reciprocal of this rate constant. When the models are fitted to similar half-times, then, it is not unexpected that the 6 and 2% models would exhibit similar values for the endocytosis rate constant, k_1. The difference in the basal PM content in the two models thus results primarily from an approximately 3-fold difference in the exocytosis rate coefficient, k_4, as well as in k_2 and k_3. Furthermore, since they are dominated by a single rate constant, the resultant half-times for both models show only a slight dependence upon the initial conditions as determined by the type of experiment. In the insulin-stimulated case, on the other hand, the relative values of k_1 and k_4 are inverted, and the endocytotic process no longer dominates the kinetics of the PM compartment (Table 1). The corresponding half-times are somewhat larger, and are much more dependent upon the type of experiment, SS or TRAN, and the associated initial conditions.

The predictions of this model analysis concerning the effect of insulin upon the kinetic coefficients for the processes of endocytosis and exocytosis are reasonably consistent with those determined by model analyses and reported in the literature (as summarized in refs *13* and *14*). The endocytotic rate constant in our model decreases by a factor of ~4, while the exocytosis coefficient increases more than 8-fold in the 6% model system, and 24-fold in the case of the 2% model. Interestingly, the other two rate coefficients involved in the system also increase in the presence of insulin, by factors between 1.8 and 6.6. This is the first demonstration of data indicating that insulin also affects the GLUT4 trafficking between discrete intracellular compartments in adipocytes.

Multicompartment models of the glucose transporter trafficking systems have been developed and analyzed by Holman et al. (*13*) and subsequently by Yeh et al. (*14*) to adequately accommodate the various observed properties of these systems. As noted by both groups, for example, the

Table 3: Characteristic Exponents for the Four-Compartment GLUT4 and GLUT1 Trafficking Models[a]

	GLUT4	GLUT1
basal (6%)	$-0.389, -0.136 \pm 0.081i$	$-4.22, -0.607 \pm 0.255i$
basal (2%)	$-0.420, -0.048 \pm 0.024i$	$-4.62, -0.665 \pm 0.279i$
insulin	$-1.114, -0.204 \pm 0.115i$	$-5.33, -1.32, -0.228$

[a] GLUT1 kinetics are based entirely upon equating the endocytosis rate coefficients for both GLUT isoforms, in both the basal and insulin-stimulated states. The complex exponent pairs correspond to oscillatory solutions, where i denotes the imaginary coefficient, $\sqrt{-1}$. These values were obtained through analytic solution of the eigenvalue equation generated by the set of three independent differential equations.

simplest two-pool model is incompatible with the different half-times observed in the insulin-stimulated state for the steady-state and transition types of experiments. This behavior is readily simulated by the three-compartment models considered by Holman et al. (*13*) and Yeh et al. (*14*), and by the four-compartment model developed here. The present model, however, possesses the advantage of being based upon experimental measurement of steady-state GLUT4 pools plausibly identified with functional compartments of the system, thus providing additional information about the relative values of the rate coefficients that are involved.

For GLUT1 trafficking, some similarity can be drawn between the results presented here and those obtained by Yeh et al. (*14*). Like these authors, we propose that GLUT1 recycles through a pathway distinct from that of GLUT4, except for a common endocytosis step (Figure 6). Unlike the resultant two-compartment configuration with one intracellular and one plasma membrane compartment for GLUT1 recycling advanced by Yeh et al. (*14*), however, the model presented here assumes a four-compartment system, based upon the observation of three distinct intracellular fractions containing GLUT1. Designation of these intracellular fractions as SR, ST, and EV compartments in Table 2 for GLUT1 is entirely arbitrary at this time, and used only for the convenience in discussion. Notably, the GLUT1 pool denoted as EV is very small in size, and represents a minor compartment if it physically exists. Should it be an analytic artifact, however, reduction of our model to the corresponding three-compartment configuration is achieved by allowing k_4 to become infinitely large, ensuring zero content in the virtual fourth compartment. Being very small in both the basal and insulin-stimulated states, EV can be eliminated with only a minor effect upon the kinetic behavior of the model.

It is interesting to note that the (mathematical) analytic solutions for the time dependence of pool contents in the model considered by Yeh et al. (*14*) were composed, in two of three cases, of a damped oscillatory solution. In our four-compartment models, the analytic solutions, with one exception, consisted of a sum of a decaying exponential and a damped oscillation, as indicated in the table of characteristic exponents (Table 3). In all cases, however, the period of oscillation is long relative to the decay time constant so that its periodic character is largely hidden in the plotted time course of the compartment distributions.

While a four-compartment model, such as the one considered here, is perhaps inadequate for faithfully representing the full complexity of the GLUT trafficking systems, it is sufficient to capture the essential features of the system, and provide a reasonable approximation of their kinetic behavior.

The model developed here is based upon steady-state distributions of GLUT4 and GLUT1 among four distinguishable fractions in rat adipocytes. Most importantly, it provides the first experimental support for the fact that insulin modulates the rate coefficients of all of the processes involved in GLUT4 recycling, acting to decrease the rate coefficient of endocytosis, while increasing all of the other rate constants. A number of biochemical and molecular biological interventions (*23−29*) are known to affect the GLUT4 recycling in adipocytes, and our kinetic analysis should be useful in identifying the site and molecular basis of the intervention. Finally, the results of the steady-state GLUT1 distribution are consistent with the hypothesis that the two GLUT isoforms share a common endocytotic process, which alone confers the insulin sensitivity of GLUT1 distribution to the plasma membrane. The validity of this hypothesis remains to be tested.

REFERENCES

1. Olefsky, J. M. (1999) *J. Biol. Chem. 274*, 1863.
2. Pessin, J. E., Thurmond, D. C., Elmendorf, J. S., Coker, K. J., and Okada, S. (1999) *J. Biol. Chem. 274*, 2593−2596.
3. Czech, M. P., and Corvera, S. (1999) *J. Biol. Chem. 274*, 1865−1868.
4. Cushman, W. W., and Wardzala, L. J. (1980) *J. Biol. Chem. 255*, 4758−4762.
5. Suzuki, K., and Kono, T. (1980) *Proc. Natl. Acad. Sci. U.S.A. 77*, 2542−2545.
6. Jhun, B. H., Rampal, A. L., Liu, H., Lachaal, M., and Jung, C. Y. (1992) *J. Biol. Chem. 267*, 17710−17715.
7. Czech, M. P., and Buxton, J. M. (1993) *J. Biol. Chem. 268*, 9187−9190.
8. Yang, J., and Holman, G. D. (1993) *J. Biol. Chem. 268*, 4600−4603.
9. Slot, J. W., Geuze, H. J., Gigengack, S., Lienhard, G. E., and James, D. E. (1991) *J. Cell Biol. 113*, 123−135.
10. Rodnick, K. J., Slot, J. W., Studelska, D. R., Hanpeta, D. E., Robinson, L. J., Gueze, H. J., and James, D. E. (1992) *J. Biol. Chem. 267*, 6278−6285.
11. Lee, W., Ryu, J. W., Souto, R. P., Pilch, P. F., and Jung, C. Y. (1999) *J. Biol. Chem. 274*, 37755−37762.
12. Martz, A., Mookerjee, B. K., and Jung, C. Y. (1986) *J. Biol. Chem. 261*, 13606−13609.
13. Holman, G. D., Leggio, L. L., and Cushman, S. W. (1994) *J. Biol. Chem. 269*, 17516−17524.
14. Yeh, J. I., Verhey, K. J., and Birnbaum, M. J. (1995) *Biochemistry 34*, 15523−15531.
15. Karnieli, E., Zarnowski, M. J., Hissin, P. J., Simpson, I. A., Salans, L. B., and Cushman, S. W. (1981) *J. Biol. Chem. 256*, 4772−4777.
16. Clark, A. E., Holman, G. D., and Kozka, I. J. (1991) *Biochem. J. 278*, 235−241.
17. Satoh, S., Nishimura, H., Clark, A. E., Kozka, I. J., Vannucci, S. J., Simpson, I. A., Quon, M. J., Cushman, S. W., and Holdman, G. D. (1993) *J. Biol. Chem. 268*, 17820−17829.
18. Mellman, I. (1996) *Annu. Rev. Cell Dev. Biol. 12*, 575−625.
19. Chakrabarti, R., Buxton, J., Joly, M., and Corvera, S. (1994) *J. Biol. Chem. 269*, 7926−7933.
20. Ceresa, B. P., Kao, A. W., Santeler, S. R., and Pessin, J. E. (1998) *Mol. Cell. Biol. 18*, 3862−3870.
21. Al-Hasani, H., Hinck, C. S., and Cushman, S. W. (1998) *J. Biol. Chem. 273*, 17504−17510.
22. Clark, A. E., Holman, G. D., and Kozka, I. J. (1991) *Biochem. J. 278*, 235−241.

Lee et al.

23. Livingstone, C., James, D. E., Rice, J. E., Hanpeter, D., and Gould, G. W. (1996) *Biochem. J. 315*, 487−495.

24. Okada, T., Kawano, Y., Sakakibara, T., Hazeki, O., and Ui, M. (1994) *J. Biol. Chem. 269*, 3568−3573.

25. Rampal, A. L., Jhun, B. H., Kim, S., Liu, H., Manka, M., Lachaal, M., Spangler, R. A., and Jung, C. Y. (1995) *J. Biol. Chem. 270*, 3938−3943.

26. Kohn, A. D., Summers, S. A., Birmbaum, M. J., and Roth, R. A. (1996) *J. Biol. Chem. 271*, 31372−31378.

27. Standaert, M. L., Galloway, L., Kamam, P., Bandyopadhyay, G., Moscat, J., and Farese, R. V. (1997) *J. Biol. Chem. 272*, 30075−30082.

28. Lee, W., and Jung, C. Y. (1997) *J. Biol. Chem. 272*, 21427−21431.

29. Lee, W., Samuel, J. S., Zhang, W., Rampal, A. L., Lachaal, M., and Jung, C. Y. (1997) *Biochem. Biophys. Res. Commun. 240*, 409−414.